Structural Studies of Two Mutants of Amicyanin from *Paracoccus denitrificans* That Stabilize the Reduced State of the Copper[†,‡]

Christopher J. Carrell,[§] Dapeng Sun,[||] Shoulei Jiang,[||] Victor L. Davidson,[||] and F. Scott Mathews*[,§]

Department of Biochemistry and Molecular Biophysics, Washington University School of Medicine, St. Louis, Missouri 63110, and Department of Biochemistry, University of Mississippi Medical School, Jackson, Mississippi 39216

Received February 18, 2004; Revised Manuscript Received May 7, 2004

ABSTRACT: Mutation of Pro94 to phenylalanine or alanine significantly alters the redox properties of the type I copper center of amicyanin. Each mutation increases the redox midpoint potential (E_m) value by at least 140 mV and shifts the pK_a for the pH dependence of the E_m value to a more acidic value. Atomic resolution (0.99−1.1 Å) structures of both the P94F and P94A amicyanin have been determined in the oxidized and reduced states. In each amicyanin mutant, an electron-withdrawing hydrogen bond to the copper-coordinating thiolate sulfur of Cys92 is introduced by movement of the amide nitrogens of Phe94 and Ala94 much closer to the thiolate sulfur than in wild-type amicyanin. This is the likely explanation for the much more positive E_m values which result from each of these mutations. The observed decrease in the pK_a value for the pH dependence of the E_m value that is seen in the mutants seems to be correlated with steric hindrance to the rotation of the His95 copper ligand which results from the mutations. In wild-type amicyanin the His95 side chain undergoes a redox and pH-dependent conformational change which accounts for the pH dependence of the E_m value of amicyanin. The reduced P94A amicyanin exhibits two alternate conformations with the positions of the copper 1.4 Å apart. In one of these conformations, a water molecule appears to have replaced Met98 as a copper ligand. The relevance of these structures to the electron transfer properties of P94F and P94A amicyanin are also discussed.

Amicyanin (*1*) is an obligatory intermediate in the transfer of electrons from methylamine dehydrogenase (MADH)[1] (*2*) to *c*-type cytochromes in *Paracoccus denitrificans* (*3*). Crystal structures are available for amicyanin (*4*) as well as complexes of amicyanin with MADH (*5*) and with both MADH and cytochrome *c*-551i (*6*), its natural electron acceptor. Amicyanin is a type I blue copper protein having a redox midpoint potential (E_m) value of 265 mV at pH 8.0 when free in solution (*1*, *7*). This potential is pH dependent, increasing to about 330 mV at pH 6; it displays a pK_a of about 7.5 (*8*). This pH dependency has been attributed to the protonation of His95, a solvent-exposed ligand to copper. It has been observed that, upon reduction of amicyanin at acidic pH, the coordination bond between the δ-nitrogen of His95 and copper is broken and the His95 side chain rotates by 180° about the $C_\beta-C_\gamma$ bond relative to its position in oxidized amicyanin (*8*, *9*). A similar "histidine flip" phenomenon has been reported for plastocyanin (*9*). When amicyanin is in complex with MADH, its E_m value decreases to about 220 mV and is independent of pH (*8*). This appears to be caused by sequestration of the exposed edge of His95 in the hydrophobic interface of the complex with the redox and pH-dependent histidine flip restricted by steric hindrance. This results in stabilization of the histidine−copper coordination bond and facilitates the subsequent energetically unfavorable electron transfer to cytochrome *c*-551i, which has an E_m value of +195 mV (*10*).

Substitution of Pro94 of amicyanin by alanine or phenylalanine increases the redox potential of the protein at pH 8.0 from 265 to 380 and 415 mV, respectively (*7*). Furthermore, the acid dissociation constant of His95, the copper ligand, decreases from a pK_a value of 7.5 for wild-type amicyanin to about 6.3 for the P94A mutant and to a value below 5 for the P94F mutant. Pro94 resides in a portion of the amino acid sequence that contains three of the amino acid residues that provide ligands to the native type I copper center: Cys92, His95, and Met98. The rationale for introducing a mutation at the site of Pro94 was to change this ligand loop to examine the effect of relaxation of the ligand environment on the redox and electron transfer properties of the copper center. In support of this hypothesis, the entropy of reduction of amicyanin was found to increase by about 45 J/(mol K) as a result of the P94F mutation (*7*). EPR data for the P94F amicyanin also indicated diminished copper−thiolate covalency (*7*). These results suggested that the mutation introduced an electron-withdrawing hydrogen bond to the copper-coordinating thiolate sulfur of Cys92. In wild-type amicyanin, only one hydrogen bond is made to the thiolate sulfur, from the amide nitrogen of Asn54, and no hydrogen bond can be made from the backbone nitrogen at

[†] This work was supported by NSF Grants MCB-0091084 (F.S.M.) and GM41574 (V.L.D.).

[‡] Crystallographic coordinates have been deposited in the Protein Data Bank under the file names 1sfd [P94F Cu(II)], 1sfh [P94F Cu(I)], 1sf5 [P94A Cu(II)], and 1sf3 [P94A Cu(I)].

* Corresponding author. E-mail: mathews@biochem.wustl.edu. Phone: (314) 362-1080. Fax: (314) 362-7183.

[§] Washington University School of Medicine.

[||] University of Mississippi Medical School.

[1] Abbreviations: MADH, methylamine dehydrogenase; NCS, noncrystallographic symmetry; rmsd, root mean square deviation; E_m, redox midpoint potential; λ, reorganization energy; H_{AB}, electronic coupling.

10.1021/bi049634z CCC: $27.50
Published on Web 06/29/2004

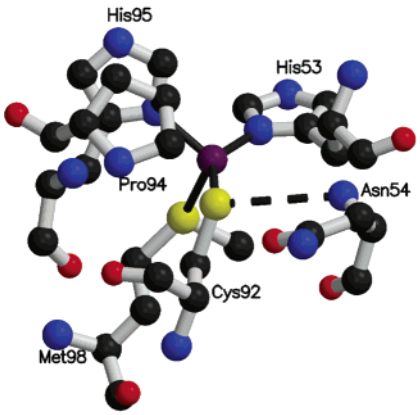

FIGURE 1: The copper center of wild-type Cu(II) amicyanin observed at pH 4.3 (pdb code 1AAC). The copper coordination bonds are denoted by solid dark gray lines, and the hydrogen bond between Asn54 and the sulfur atom of Cys92 is in dashed dark gray. This figure was prepared using Molscript (*34*) and Raster3D (*35*).

Pro94 to that thiolate sulfur (Figure 1). In other blue copper proteins such as azurin, which lack proline at this position, a second such hydrogen bond comes from the amide group of a residue close to the histidine ligand and structurally aligned with Pro94. The result of the additional hydrogen bond in amicyanin would be to weaken the bond between copper and the sulfur atom of Cys92 and thereby make the copper site less constrained.

In this paper we report the atomic resolution structures of both the P94F and P94A mutants of amicyanin in the oxidized and reduced states at pH 5.5. From this information it is possible to determine the structural basis for the observed changes in the magnitude and pH dependence of the E_m value that results from these mutations. Changes in structure are also correlated with changes in electron transfer properties in amicyanin that are caused by these mutations.

EXPERIMENTAL PROCEDURES

Protein Purification. Previously described procedures were used to purify MADH (*11*), amicyanin (*1*), and cytochrome *c*-551i (*3*) from *P. denitrificans* (ATCC 13543). P94F and P94A amicyanins were expressed in *Escherichia coli* and purified from the periplasmic fraction as described previously for other recombinant amicyanin mutants (*12*).

Crystallization and Structure Analysis. The P94F mutant of amicyanin was crystallized by the sitting drop vapor diffusion method from 100 mM sodium citrate (pH 5.5) and 2.25 M ammonium sulfate. The crystals are orthorhombic, space group $P2_12_12_1$, with cell parameters of $a = 51.0$ Å, $b = 59.5$ Å, and $c = 74.3$ Å and two molecules in the asymmetric unit. The P94A mutant crystals were grown by macroseeding using a 9-to-1 mixture of monobasic sodium (3 M) and dibasic potassium (3 M) phosphate solution as precipitant as described previously (*13*). The crystals are monoclinic, space group $P2_1$, with cell parameters $a = 28.4$ Å, $b = 55.4$ Å, $c = 27.1$ Å, and $\beta = 95.2°$. They contain one molecule per asymmetric unit and are isomorphous with crystals of the wild-type protein. Data from the dark blue oxidized mutant crystals and from colorless reduced mutant crystals that had been incubated with 10 mM sodium ascorbate in 4 M sodium/potassium phosphate buffer (in the ratio 4:1, pH ~5.5) for ~30 min were recorded at the BIOCARS beamline 14-BM-C of the Advanced Photon Source using an ADSC-Q4 CCD detector. The data were recorded at 100 K, using paratone oil (Hampton Research, Laguna Hills, CA) as a cryoprotectant, to resolutions ranging from 0.99 to 1.10 Å (see Table 1). All of the data sets were processed using DENZO and SCALEPACK (*14*). The data collection statistics are presented in Table 1.

Structures of the oxidized P94F mutant of amicyanin were solved by molecular replacement with a two-molecule search procedure using the Molrep package in CCP4 (*15*). Initial stages of refinement were performed by CNS (*16*) against data limited to 2.0 Å resolution. The model was then refined using SHELX (*17*) against data to 0.99 Å resolution, alternating cycles of least-squares refinement with model building in XtalView (*18*). Hydrogen atoms, positioned as a riding model, were included in the refinement in SHELX. The structure of the reduced form of P94F was determined by direct refinement of the oxidized structure against the reduced data, using SHELX, after prior removal of solvent molecules and alternate amino acid conformations. Both the oxidized and reduced forms of the P94A mutant were refined directly from the oxidized wild-type protein structure, again using SHELX. During refinement of all four crystal structures alternating cycles of refinement and model building in XtalView were carried out. The temperature factors of all non-hydrogen atoms were refined anisotropically. The refinement statistics can be found in Table 1.

Other Crystallographic Calculations. Buried molecular surface areas were computed using the program AREAIMOL of the CCP4 package (*15*).

Electron Transfer Reactions of P94A Amicyanin. The rates of the electron transfer reactions from *o*-quinol MADH to oxidized P94A amicyanin and from reduced P94A amicyanin to oxidized cytochrome *c*-551i were determined as described previously for study of the analogous reactions of P94F amicyanin (*19*).

RESULTS

Crystal Structure Analysis. The structures of the oxidized and reduced forms of the P94F and P94A mutants of amicyanin were determined at very high resolution, ranging from 0.99 to 1.10 Å resolution. Analysis of the structural quality using PROCHECK indicates that all of the residues are in either the most favored or additionally allowed regions of the Ramachandran plot except for the oxidized P94F amicyanin structure, in which one residue is in the generously allowed region.

Each of the structures exhibits alternate conformations for several of the amino acid side chains (Table 1). For the P94F oxidized structure, five side chains are in alternate conformations (three in subunit 1 and two in subunit 2), while for P94F reduced, seven side chains have alternate conformations (three in subunit 1 and four in subunit 2). Oxidized P94A amicyanin has four side chains in alternate conformations whereas the reduced P94A contains eight side chains plus a complete eight-residue polypeptide segment in alternate conformations plus two alternate positions for the copper ion. Oxidized P94F also contains five sulfate anions while reduced P94F contains two sodium ions and reduced P94A contains two phosphate anions. In addition, the sulfur atom of Met51 in oxidized P94A appears to be oxidized to

Table 1: Data Collection and Refinement Statistics

sample	P94F Cu(II)	P94F Cu(I)	P94A Cu(II)	P94A Cu(I)
data collection				
wavelength (Å)	0.9000	0.9000	0.9000	0.9000
space group	$P2_12_12_1$	$P2_12_12_1$	$P2_1$	$P2_1$
a (Å)	51.03	51.43	28.40	28.41
b (Å)	59.50	59.67	55.43	55.56
c (Å)	74.35	74.35	27.10	27.12
α (deg)	90	90	90	90
β (deg)	90	90	95.17	95.98
γ (deg)	90	90	90	90
max resolution (outer shell) (Å)	0.99 (1.01−0.99)	1.05 (1.07−0.105)	1.10 (1.12−1.10)	1.05 (1.07−1.05)
$I/\sigma(I)$[a]	32.5 (6.8)	26.1 (2.9)	24.5 (2.8)	33.0 (3.6)
no. of observations	976228	891880	152193	155365
no. of unique reflections	100793	98032	32824	35890
% completion (outer shell)	79.7 (63.1)	91.6 (64.7)	96.7 (71.5)	91.7 (52.5)
redundancy	9.7	9.1	4.7	4.3
R_{merge}[b] (outer shell)	0.057 (0.381)	0.083 (0.243)	0.056 (0.323)	0.036 (0.221)
refinement				
data range (Å)	30−0.99	30−1.05	30−1.10	30−1.05
no. of reflections	97220	97974	32770	35854
R^c_{work}	0.116	0.122	0.127	0.117
R^c_{free}	0.147	0.153	0.166	0.147
R^c_{total}	0.119	0.124	0.130	0.119
test set fraction (%)	8.0	8.0	8.0	8.0
hydrogen atom model	riding	riding	riding	riding
no. of protein atoms	1637	1650	823	897
no. of copper ions	2	2	1	2
no. of ion atoms (SO_4^-, PO_4^-, Na^+)	30	2	0	10
no. of solvent molecules	487	409	153	151
residues in alternate conformation	Ser9A, Met71A, Lys101A, Met71B, Lys101B	Lys68A, Met71A, Glu84A, Ser9B, Glu15B, Met71B, Glu84B	Ser9, Met28, Lys29, Asp89	Lys2, Ser9, Glu15−Val22, Met28, Lys38, His53, Met71, Asp89, His95, Cu^+
$\langle B \rangle$ protein atoms (Å^2)	9.8	12.6	13.5	12.3
$\langle B \rangle$ anion atoms (Å^2)	24.2	26.3		33.2
$\langle B \rangle$ solvent atoms (Å^2)	26.6	27.7	28.0	27.2
rms ΔB (m/m, Å^2)[d]	1.6	2.1	1.7	1.6
rms ΔB (m/s, Å^2)[d]	2.4	2.4	2.6	2.2
rms ΔB (s/s, Å^2)[d]	4.8	5.5	3.9	4.3
estimated coordinate error (Å)				
Luzzati[e]	0.155	0.114	0.127	0.118
DPI[f]	0.043	0.033	0.045	0.045

[a] $I/\sigma(I)$ is the average signal-to-noise ratio for merged reflection intensities. [b] $R_{merge} = \sum_h \sum_i |I(h) - I_i(h)| / \sum_h \sum_i I_i(h)$, where $I_i(h)$ is the *i*th measurement and $I(h)$ is the mean measurement of reflection *h*. [c] $R = \sum_h |F_o - F_c| / \sum_h |F_o|$, where F_o and F_c are the observed and calculated structure factor amplitudes of reflection *h*. R_{free} is *R* for the test reflection data set for cross-validation of the refinement (*31*), R_{work} is *R* for the working reflection set, and R_{total} is *R* for all of the data. [d] Root mean square difference in *B*-factor for bonded atoms; m/m, m/s, and s/s represent main chain−main chain, main chain−side chain, and side chain−side chain bonds, respectively. [e] Based on the Luzzati plot (*32*) of *R* vs 2 sin θ/λ, where θ is the angle of diffraction and λ is the X-ray wavelength. [f] DPI is the diffraction data precision indicator (*33*) based on *R* or R_{free} and a rough approximation to the least-squares method.

the sulfoxide and has been modeled with an oxygen atom covalently attached to it.

Structure of Oxidized P94F Amicyanin. Unlike wild-type amicyanin, the crystals of the P94F mutant contain two protein molecules in the asymmetric unit. The two molecules are related by a noncrystallographic 2-fold axis and are linked by a symmetric pair of hydrogen bonds between the His95 NE2 atom of one molecule and the Phe94 carbonyl oxygen of the other (Figure 2). In addition there are hydrophobic interactions among the side chains of Met51, Pro52, Lys68, Met71, Thr93, Phe94, His95, and Pro96 between the two molecules. The planes of the Phe96 side chain rings are parallel, approaching to within 3.6 Å of each other, but the rings do not overlap. The surface area that becomes buried through the interaction of the two molecules within the crystal is about 300 Å^2 for each molecule. It should be noted that these protein−protein interactions are very possibly a consequence of the crystallization conditions since there is no evidence for dimer formation of P94F amicyanin in solution.

A comparison of the two molecules of oxidized P94F amicyanin in the asymmetric unit (Figure 3) shows a root mean square deviation (rmsd) of Cα positions of 0.59 Å over the entire 105-residue polypeptide chain. The regions of highest deviation are residues 1−8 (1.35 Å rmsd), 14−19 (1.09 Å rmsd), and 61−64 (0.94 Å rmsd), with another region of lower deviation (0.55 Å rmsd) in segment 49−52. In the first three of these regions one molecule is in close crystal contact with a neighboring molecule while the other molecule is not; in the fourth region (segment 49−52) both molecules in the asymmetric unit make nearly symmetrical crystal contact with each other. These four segments are located within surface loops of the protein and connect *β*-sheet elements of secondary structure. Such loops are likely to maintain some flexibility.

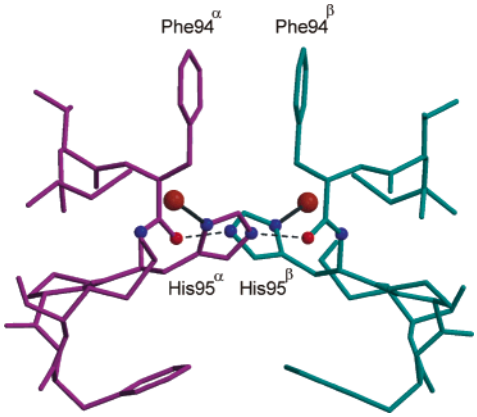

FIGURE 2: 2. Intermolecular contact between Phe94 and His95 in the oxidized P94F mutant crystal. The polypeptide chains for residues Cys92−Phe97 for the two molecules in the asymmetric unit are drawn as stick figures in violet and cyan. Hydrogen bonds (dashed lines) are formed between the NE2 atom (blue circles) of each His95 and the carbonyl O atom (red circles) of each Phe94 of the other molecule. The coordination bonds (solid lines) between ND1 of each histidine and the copper ion (brown circle) are also shown. The figure was rendered using XtalView (*18*) and Raster3D (*35*).

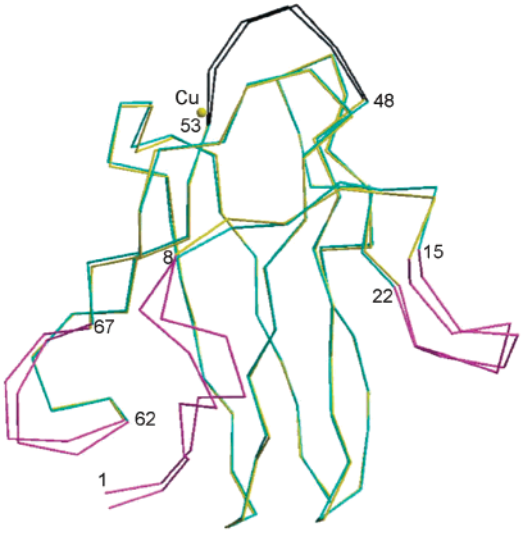

FIGURE 3: 3. Molecule 2 (cyan) of P94F amicyanin superposed on molecule 1 (yellow). The N-terminal region (Asp1−Glu8), the loop between Ala15 and Val22, and the loop between Leu62 and Leu67 are in magenta, and the loop between Arg48 and His53 is in black. This figure was rendered with XtalView (*18*) and Raster3D (*35*).

When the P94F mutant is compared to the wild-type amicyanin, deviations in Cα position also occur within the first three segments described above where the two P94F molecules differ substantially from each other. These deviations probably result from differences in intermolecular contacts. In addition, significant side chain and some main chain movements, which are not observed in the wild-type structure, occur at Met51, Pro52, Met71, and Pro/Phe94. The structural changes at Pro/Phe94 and Met71 appear to be directly related to the P94F mutation within the molecule (Figure 4a). The Cα atom at position 94 moves 0.82 Å on replacement of Pro with Phe while Cα atoms on either side move about 0.23 Å; the peptide backbone conformational angles (ϕ, ψ) change from (−73, −13) for Pro94 to (−70, −32) for Phe94. As a result, the amide nitrogen of Phe94, now protonated, moves about 0.7 Å closer to Cys92 SG than in the wild-type protein and is capable of forming a new hydrogen bond to it (Figure 4b). The Phe94 N−Cys92 SG distance is now 3.53 Å compared to that of Asn54 N−Cys92 SG of 3.56 Å (Table 2). Based on modeled hydrogen positions (see Experimental Procedures), the N−H−S bond angle at Phe94 is 131° compared to 163° for the angle at Asn54, leading to estimated S−H distances of 2.91 Å for Phe94 compared to 2.73 Å for Asn54.

In addition to these changes at the active site, the side chain of Phe94 extends 3.79 Å beyond the tip of the proline ring it displaces and occupies space previously taken up by the Met71 side chain (Figure 4b). Because of this, the latter side chain is reoriented away from its former position by a movement of 5.85 Å of its CE atom. The structural changes at Met51 and Pro52 appear to be an indirect effect of the P94F mutation (Figure 4a). The Met51 CE side chain atom moves 1.78 Å to avoid a close contact with T93′ O of the 2-fold noncrystallographic symmetry (NCS) related molecule (where the prime indicates the other molecule) while the Pro52 CG atom moves 0.66 Å closer to the 2-fold NCS-related molecule to improve the packing with the Phe94′ side chain. The final orientation of the Met71 side chain may also be affected by interaction with the Met71′ side chain of the 2-fold NCS-related molecule.

Structure of Reduced P94F Amicaynin. There appears to be no discernible difference between the structures of oxidized and reduced P94F amicyanin. Comparison of their structures, utilizing the full asymmetric unit, shows an rmsd for 210 equivalent Cα atoms of 0.16 Å. These structures were both determined at pH 5.5, which is below the observed pK_a of wild-type amicyanin but above the observed pK_a of P94F amicyanin (*7*). The copper atom itself might be expected to change position on reduction to the Cu(I) state, even in the absence of a histidine flip, which is not seen in the P94F amicyanin structure. One possible explanation for the observed lack of change in position of the copper center of P94F amicyanin on reduction (Table 3) may be found in the close intermolecular crystal contacts between the 2-fold NCS-related molecules in the asymmetric unit, as described above, which involve several residues close to the copper-binding ligands. However, it is unlikely that these interactions occur in solution. As discussed later, it is more likely that the observed changes in the pH dependence of P94F amicyanin may instead be due to steric restraint to the histidine flip caused by the presence of Phe at position 94.

Structure of Oxidized P94A Amicyanin. The oxidized P94A structure is virtually the same as that of wild-type amicyanin. The rmsd of Cα atoms between the two structures is 0.44 Å, which drops to 0.29 Å when the highly flexible segment 18−20 is omitted. The Cα atom at position 94 moves by 0.5 Å when Pro is replaced by Ala while those at positions 93 and 95 remain within about 0.2 Å of the wild-type position. The changes in the polypeptide conformational angles (ϕ, ψ) for the P94A mutation are about the same as for the P94F mutation. The new Ala94 amide to Cys92 SG hydrogen bond, observed in the P94F mutant, is present in the P94A mutant with similar geometry (Table 2).

Structure of Reduced P94A Amicyanin. Unlike P94F amicyanin, the P94A mutant shows significant structural differences upon reduction to the Cu(I) state. As mentioned above, 16 residues plus the copper atom of reduced P94A are in alternate conformations. Conformation A, the "major"

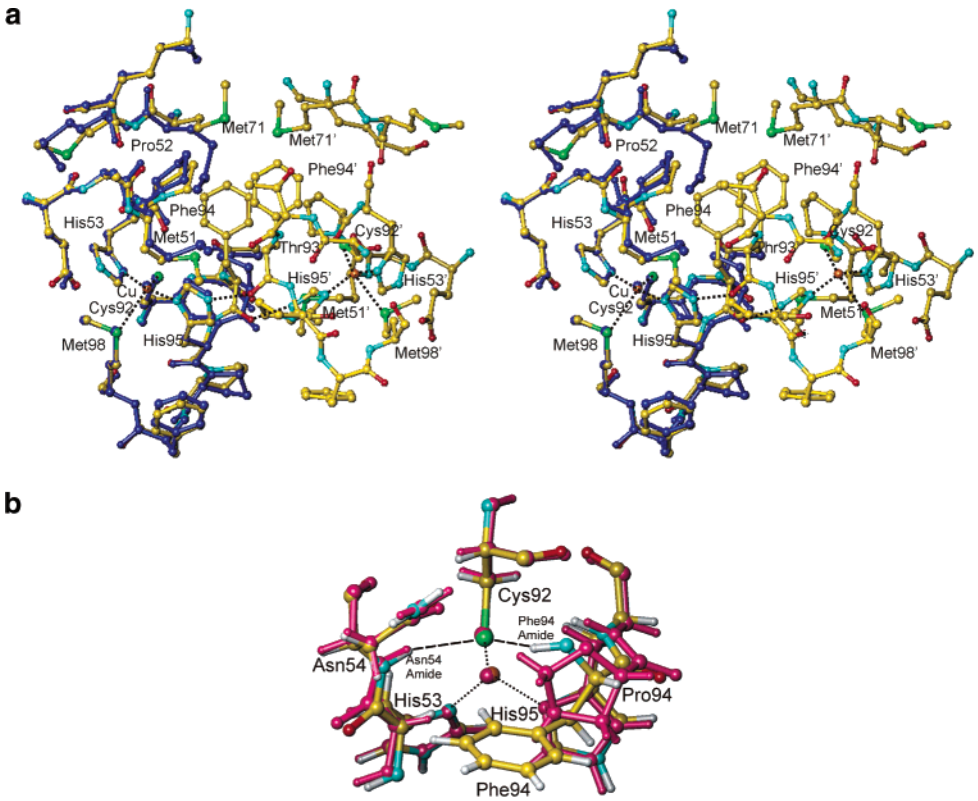

FIGURE 4: (a) Stereoview near the copper site of a comparison of molecule 1 of the P94F mutant (atom colors: carbon, yellow; oxygen, red; nitrogen, cyan; sulfur, green) with the native wild-type amicyanin (blue) and of the interactions between molecules 1 and 2 of the mutant. Residues that show significant changes in side chain orientation or interactions between molecules are labeled. The copper ion and its four ligands are also labeled, and the coordination bonds are shown as dashed lines. The hydrogen bonds between atom NE2 of His95 and the carbonyl oxygen of Phe94 are also shown as dashed lines. (b) Monoview of the copper-binding site of P94F amicyanin superimposed on that of the wild-type protein. Residues His53, Asn54, Cys92, Pro/Phe94, and His95 and the copper atom are shown, along with the predicted hydrogen atoms. The P94F mutant is shown in atom colors as in panel a, plus hydrogen atoms in white, and the native wild-type amicyanin is in violet. The two peptide amide hydrogen bonds from Asn54 and Phe/Pro94 are shown as dashed lines, and the coordination bonds from copper to His53, Cys92, and His95 are shown as dotted lines. These diagrams were prepared using Turbo-Frodo (*36*).

Table 2: Hydrogen Bonds between the Sulfur of Cys92, a Copper Ligand, and Nearby Peptide Amide Groups in Wild-Type and Mutant Amicyanin and Comparisons to Analogous Hydrogen Bonds in Plastocyanin, Pseudozurin, and Azurin

	amicyanin[a]			azurin[b]	plastocyanin[c]	pseudoazurin[d]		
	wild type	P94A[e]	P94F[f]	wild type	wild type	wild type	P80A[g]	P80I[h]
amide 1 N−Cys SG (Å)[i]	3.64	3.70 (0.06)	3.56 (0.02)	3.57	3.58	3.61	3.68 (0.03)	3.56 (0.04)
amide 1 H−Cys SG (Å)[i]	2.67	2.84 (0.06)	2.73 (0.02)	2.62	2.53	2.65	2.74 (0.04)	2.58 (0.03)
angle N−H−SG (deg)	165	171 (0.8)	163 (2.3)	158	166	161	155 (0.7)	165 (1.4)
amide 2 N−Cys SG (Å)[j]		3.82 (0.03)	3.53 (0.02)	3.44			3.56 (0.14)	3.58 (0.08)
amide 2 H−Cys SG (Å)[10]		3.19 (0.01)	2.91 (0.04)	2.46			2.84 (0.19)	2.90 (0.12)
angle N−H−SG (deg)		134 (2.2)	131 (1.4)	165			130 (4.2)	127 (2.8)

[a] Amide 1 is Asn54, and amide 2 is Pro94; wild type PDB code 1aac; resolution 1.3 Å. [b] Amide 1 is Asn47, and amide 2 is Phe114; PDB code 1jzf; resolution 1.5 Å. [c] Amide 1 is Asn38; PDB code 1plc; resolution 1.33 Å. [d] Amide 1 is Asn41, and amide 2 is Pro80; wild type PDB code 1paz; 1.55 Å resolution. [e] Values averaged over oxidized and reduced structures of P94A. Numbers in parentheses are the mean deviation from the average. For comparison, the standard deviation of the nitrogen to sulfur bond distances based on the estimated errors in coordinates is 0.023 Å. [f] Values averaged over oxidized and reduced structures of P94F. Numbers in parentheses are the mean deviation from the average. For comparison, the standard deviation of nitrogen to sulfur bond distances based on the estimated errors in coordinates is 0.014 Å. [g] Values averaged over oxidized and reduced structures of P80A, PDB codes 4paz (resolution 1.76 Å) and 5paz (resolution 1.76 Å). Numbers in parentheses are observed standard deviations. [h] Values averaged over oxidized and reduced structures of P80I, PDB codes 6paz (resolution 1.91 Å) and 7paz (resolution 1.75 Å). Values in parentheses are the mean deviation from the average. [i] Amide 1 refers to the peptide amide with lower sequence number that is hydrogen bonded to the SG atom of the cysteine copper ligand. [j] Amide 2 refers to the peptide amide with higher sequence number that is hydrogen bonded to the SG atom of the cysteine copper ligand.

one, does not differ greatly from the oxidized form of the mutant, displaying an rmsd of 0.16 Å for 105 equivalent Cα positions. Conformation B differs from conformation A in two regions, one close to the copper (Cα within 5 Å, category 1) and one distant from the copper (Cα farther than 5 Å, category 2). Residues in the second category, distant from the copper, include the complete polypeptide segment 15−22 and an additional six side chains and range in relative occupancy from 0.28 to 0.51. Although segment 15−22 probably moves as a unit, there is no way to correlate the conformation of that segment nor the other remaining alternate side chain conformations of this category with each other, nor with the atoms of category 1, and their assignment to one or the other "conformation" is arbitrary. In contrast,

Table 3: Copper Coordination Distances in Oxidized (ox.) and Reduced (red.) P94F and P94A Mutants Compared with Wild-Type and Cobalt-Substituted Amicyanin

	P94F ox.	P94F red.	P94A ox.	P94A red. (conf A)	P94A red. (conf B)	WT ox. (pH 4.8)[a]	WT red. (pH 4.4)[b]	cobalt amicyanin[c]
M[d]−His53 ND1 (Å)	1.98	1.98	2.05	1.89	2.24	1.96	1.91	2.06
M[d]−Cys92 SG (Å)	2.22	2.20	2.04	2.09	2.14	2.08	2.09	2.19
M[d]−His95 ND1/CD2 (Å)	2.05	2.03	2.07	3.25	2.02	2.03	3.51	1.93
M[d]−Met98 SD (Å)	2.75	2.89	3.15	3.01	3.94	2.91	2.9	3.76
M[d]−water (Å)					2.12			2.26

[a] Reference *4*. [b] Reference *8*. [c] Reference *37*. [d] M refers to the copper ion in all cases except the cobalt-substituted amicyanin presented in the last column.

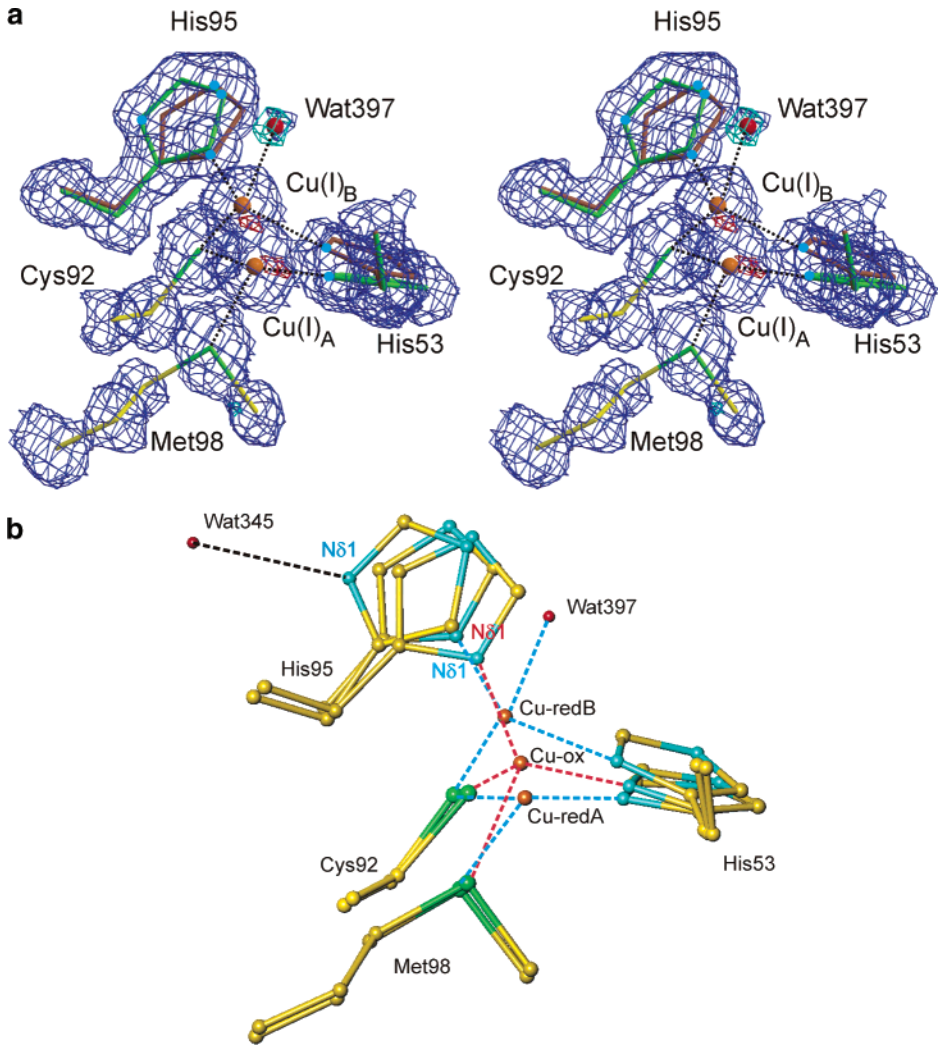

FIGURE 5: (a) Stereoview of the reduced P94A amicyanin mutant superimposed on the $2|F_o| - |F_c|$ and $|F_o| - |F_c|$ electron density maps contoured at 1σ (blue) and $\pm 4\sigma$ (cyan and red), respectively. The small bit of positive $|F_o| - |F_c|$ density (cyan) above the copper structure was interpreted and refined as a partially occupied water molecule, Wat397, coordinated to the partially occupied copper(I) ion site (Cu_B) in the upper position. His53 and His95 in conformations 1 and 2 are depicted as green sticks and brown sticks, respectively, with the ND1 and NE2 atoms as cyan circles. The coordination bonds between copper(I) ions Cu_A and Cu_B (brown) and its ligands are shown as dashed lines. The figure was rendered using XtalView (*18*) and Raster3D (*34*). (b) The reduced state of the amicyanin mutant P94A superposed on the oxidized state. The copper structure of reduced P94A is built as two partially occupied atoms, labeled Cu-redA and Cu-redB, 1.4 Å apart. The copper in the oxidized state is labeled Cu-ox. The coordination bonds between the ligand side chains and the copper are drawn as dashed lines, blue for the reduced forms of the protein in conformations A and B and red for oxidized forms. This diagram was prepared using Turbo-Frodo (*36*).

the residues in the first category, close to the copper, appear to be highly correlated and consist of residues His53 and His95 and the copper. The two alternate copper positions are 1.41 Å apart (Figure 5a). In conformation A (with relative occupancy 0.58) the copper has moved closer to the SD atom of Met98 by about 0.15 Å and is tridentate, coordinated by His53 ND1, Cys92 SG, and Met98 SD (Table 3, Figure 5b). The side chain of His95 appears to have "flipped" so that the CD2 atom is 3.24 Å away from the copper and a water molecule, Wat345, forms a hydrogen bond to its ND1 atom (Figure 5b). This conformation thus closely resembles that of the reduced wild-type amicyanin at pH 4.4 (*8*). In conformation B, the copper has moved in the opposite direction and is farther from Met98 SD by 0.80 Å. Although

Table 4: Electron Transfer Rate Constants and Parameters for the Reactions of Wild-Type and Mutant Amicyanins with MADH and Cytochrome *c*-551i

	wild type[a]	P94F[b]	P94A
electron transfer from MADH			
k_{ET} (s^{-1}) at 30 °C	9.8	60	82
$\Delta G°$ ($J \cdot mol^{-1}$)	−3184	−21710	−18240
λ (eV)	2.3 ± 0.1	2.3 ± 0.1	nd[c]
H_{AB} (cm^{-1})	12 ± 7	4.6 ± 1.3	nd
electron transfer to cyt *c*-551i			
k_{ET} (s^{-1}) at 30 °C	87	0.56	0.39
$\Delta G°$ ($J \cdot mol^{-1}$)	3184	21710	18240
λ (eV)	1.2 ± 0.1	1.3 ± 0.1	nd
H_{AB} (cm^{-1})	0.3 ± 0.1	0.3 ± 0.1	nd

[a] References *29* and *30*. [b] Reference *28*. [c] nd, not determined.

the conformation B copper appeared at first to be tridentate, coordinated by His53 ND1, Cys92 SG, and His95 ND1 (Table 3), a small peak was observed in the $|F_o| - |F_c|$ difference map close to the copper site (Figure 5a) and indicated that a water molecule is bound at this position to form a fourth ligand to the Cu(I) ion. This water was included in the final stages of refinement and has a lower than average thermal *B*-factor of 16 Å^2 (Table 1) and an occupancy of 0.42, the same as the minor conformers of His53, His95, and copper. The coordination geometry of the minor copper site is presented in Table 3 and Figure 5b. This 4-fold coordination to a metal ion employing a water molecule has not previously been reported for a native or mutant type I copper protein. However, a similar coordination involving a water molecule has also been observed in a cobalt-substituted form of amicyanin (*37*).

Electron Transfer to and from P94A Amicyanin. The rates of the electron transfer reactions from *o*-quinol MADH to oxidized P94A amicyanin and from reduced P94A amicyanin to oxidized cytochrome *c*-551i are listed in Table 4 and compared with the previously reported electron transfer rates of wild-type and P94F amicyanins.

DISCUSSION

Lowering of the pK_a of His95 Protonation in P94 Mutants of Amicyanin. There are two major effects of mutating residue Pro94 to Ala or Phe. One is to lower the pK_a of the protonation of His95 to values near 6.3 and below 5, respectively (*7*). The other is to increase in E_m values of these two mutants by 115−150 mV with respect to the wild-type protein.

In the wild-type amicyanin crystal, the side chain of His95 makes contact only with solvent and is relatively free to move upon reduction of Cu(II) to Cu(I) (*4*). In the P94F crystal, His95 is involved in a tight hydrogen-bonding interaction with a second P94F amicyanin molecule related by a local 2-fold axis. When the crystal of P94F amicyanin is reduced by ascorbate, His95 is not free to move because of these interactions, and therefore the coordination bond to the copper cannot be broken without disrupting the crystal. Thus, the crystal lattice interactions prevent the observation of any conformational effects of reduction of P94F amicyanin that might occur in solution.

The P94F and P94A structures do, however, suggest a possible contributing factor leading to kinetic stabilization of the nonprotonated form of His94 in the reduced proteins. In wild-type amicyanin His95 is relatively free to rotate about the Cβ−Cγ bond, with the closest approach between atom ND1 of His95 and CB of Pro94 being 3.1 Å (Figure 6). In the P94A mutant this approach distance to CB of Ala94 is reduced to 2.8 Å, and in the P94F mutant the approach distance of CB of Phe94 is further reduced to 2.6 Å. The increase in the steric hindrance to the rotation of His95 in the wild type and P94A and P94F mutants, to the extent reflected by the decrease in the minimal ND1 to CB distances of 3.1, 2.8, and 2.6 Å, respectively, correlates well with the observed lowering of the pK_a of His95 protonation of 7.5, 6.3, and <5.0.

Hydrogen Bonding of the Cysteine Ligand to Copper. In all cupredoxins there is a conserved hydrogen bond between the amide nitrogen of a conserved asparagine side chain and the sulfur atom of the cysteine ligand to the copper (*20*). The conserved asparagine is located just beyond the first histidine ligand to copper (Asn54 in the case of amicyanin), and the hydrogen bond is indicative of the fact that the sulfur atom bound to copper is a thiolate (*21*). The nitrogen−sulfur distance is about 3.6 Å, and the N−H distance and N−H−S angle (based on the expected hydrogen position) are about 2.5−2.6 Å and 160−165°, respectively (Table 2). In azurin, there is a second hydrogen bond of similar geometry between the thiolate sulfur and an amide nitrogen (of residue Phe114 in azurin from *Pseudomonas aeruginosa*, Table 2) located about halfway in sequence between the cysteine and the second histidine copper ligand. In amicyanin, Pro94 is equivalent in position to Phe114 of azurin and cannot form a hydrogen bond involving its amide nitrogen. In pseudoazurin (*22*) and plastocyanin (*9*) this hydrogen bond is also absent, the analogous residue also being proline.

It has been postulated (*7*, *23*) that this second hydrogen bond to the thiolate sulfur, if it could form, would favor an increase in the redox potential of the copper. This could arise through delocalization of the negative charge on the thiolate sulfur which would help to stabilize the reduced state of the copper ion. It should be noted that while azurin possesses such a hydrogen bond, its E_m value is somewhat more positive than that of amicyanin but not as positive as the P94F and P94A mutants, ranging from 293 mV at pH 8.0 to 346 mV at pH 5.0 (*24*). This may be related to the fact that the backbone oxygen of Gly45 in azurin is oriented such that it provides a "fifth" ligand for copper (*25*) and makes the copper site more constrained relative to that of amicyanin. In the P94F and P94A mutants of amicyanin (Table 3), the amide nitrogens of Phe94 and Ala94 are located nearly as close to the thiolate (3.5−3.8 Å), but the angle of the putative hydrogen bond is less optimal. When hydrogen atoms are placed at their expected positions, the average hydrogen to sulfur distance is 2.9 Å for P94F and 3.2 Å for P94A, and in both the N−H−S angle is about 132°. These distances suggest that the Ala94 amide hydrogen bond to the thiolate would be weaker than that of Phe94, consistent with the more positive E_m value of the latter.

In pseudoazurin, a pair of mutations at Pro80, the equivalent of Pro94 in amicyanin, have been made, one to Ala and the other to Ile (*26*). These mutations result in increases in E_m value of 140 and 180 mV, respectively, over the wild-type protein. The crystal structures of these two mutants (*26*) also indicate that a second hydrogen bond, from the amide of residue 80 to the thiolate, may form, since the

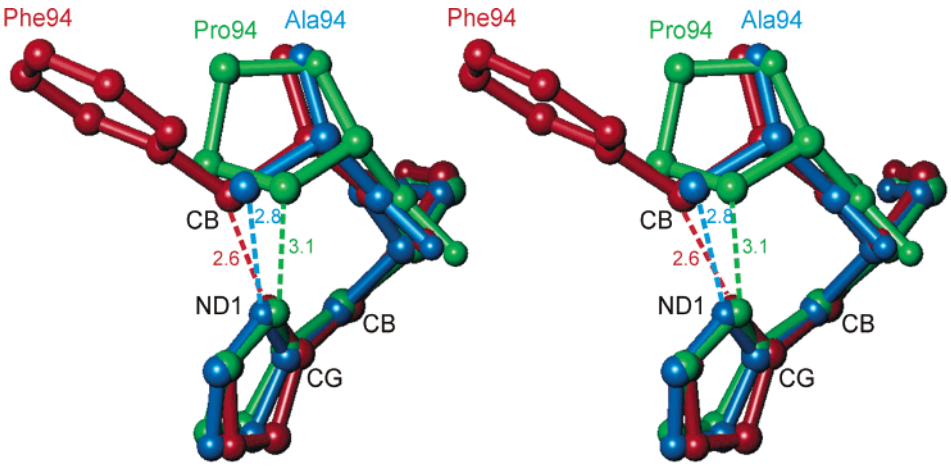

FIGURE 6: Stereoview showing the closest contacts (dashed lines) between the ND1 atom of His95 and the CB atoms of the residue at position 94 in the wild-type (green, proline), P94A (blue, alanine), and P94F (red, phenylalanine) amicyanin structures. In each case His95 has been rotated about its CB−CG bond so as to minimize the distance between atom ND1 of histidine and atom CB of the residue at position 94. The distances shown are in angstroms. This diagram was prepared using Turbo-Frodo (*36*).

postulated hydrogen to sulfur distance averages about 2.9 Å. In this case the expected strength of the hydrogen bond is about the same for the two mutants, although the resolution of the pseudoazurin mutant structures, 1.7−2.0 Å, is somewhat lower than that of the amicyanin mutant structures reported here (1.0−1.1 Å). One complicating aspect of the P80A pseudoazurin structure is the presence of a water molecule that occupies part of the vacant proline site and is also hydrogen bonded to the amide nitrogen of Ala80 and the side chain of Asn41. In the P94A structure of amicyanin, no additional water is bound to the equivalent site.

Geometry of the Copper-Binding Loop. Since the P94F amicyanin crystallizes as a dimer, it is not possible to know whether changes in conformation in the copper ligand loop may occur in solution that are suppressed in the crystalline state by the presence of the second protein in the dimer. However, the structure of the P94A amicyanin mutant is monomeric in the crystalline state and reveals that the copper structure in the reduced form is less constrained than in the wild-type amicyanin. Multiple conformations for both histidine ligands as well as the copper site are observed in reduced P94A amicyanin. Wild-type amicyanin reduced at pH 7.7 and refined at 1.30 Å resolution shows evidence for two conformations for residue His95 and the copper ion, corresponding to the flipped and unflipped forms of the molecule (*8*). The major copper position in Cu(I) P94A amicyanin is consistent with the flipped form found in the pH 7.7 reduced amicyanin. In contrast, the minor position is in a quite different position from the second position in wild-type Cu(I) amicyanin. This minor position in Cu(I) P94A amicyanin is also accessible to solvent, as evidenced by the presence of a water molecule that coordinates to the minor site copper atom.

Relevance to Electron Transfer Properties. The electron transfer reactions of *P. denitrificans* amicyanin with its physiologic electron donor, MADH, and acceptor, cytochrome *c*-551i, have been extensively studied. These reactions have been analyzed by electron transfer theory (*27*), and the reorganization energy (λ) and electronic coupling (H_{AB}) associated with each reaction have been determined (*28*−*30*). Analogous studies have been performed with P94F amicyanin (*19*). It was observed that, compared to the native system, the electron transfer rate (k_{ET}) from MADH to P94F amicyanin was much greater and the k_{ET} from P94F amicyanin to cytochrome *c*-551i was much slower (Table 4). The changes in k_{ET} were consistent with the predictions of Marcus theory of the dependence of k_{ET} on driving force and suggested that the P94F mutation had little, if any, effect on electron transfer parameters other than the change in E_m value. Thermodynamic analysis of these electron transfer reactions revealed that the values of λ for the electron transfer reactions were unaffected by the mutation (Table 4). The H_{AB} for the electron transfer from amicyanin to the cytochrome was unaffected by the P94F mutation. The H_{AB} for the electron transfer from MADH to amicyanin was slightly lower and likely reflects subtle changes at the MADH−amicyanin interface caused by the P94F mutation that affect the interprotein distance segment of the electron transfer path from TTQ to copper. These data indicate that while the P94F mutation significantly affects the relative stabilization of the oxidized and reduced states of copper in amicyanin, it has essentially no effect on the magnitude of the reorganization energy for the ET reactions of the type I copper center.

Preliminary examination of the electron transfer reactions of P94A amicyanin with MADH and cytochrome *c*-551i reveals that the electron transfer rates to and from copper have also been altered by the P94A mutation (Table 4). As was observed with P94F amicyanin, the k_{ET} from MADH to P94A amicyanin was much greater, and the k_{ET} from P94A amicyanin to cytochrome *c*-551i was much less than for the reactions with wild-type amicyanin. However, the k_{ET} from MADH to P94A amicyanin was greater than that of P94F amicyanin, and the k_{ET} from P94A amicyanin to cytochrome *c*-551i was less than that with P94F amicyanin. This was unexpected since the E_m value of P94A amicyanin is less positive than that of P94F amicyanin. This suggests that other kinetic or electron transfer parameters may have been altered by the P94A mutation. This would be consistent with the more extensive structural changes that were observed for the reduced structures of P94A amicyanin relative to P94F amicyanin. Further studies of the thermodynamics of the electron transfer reactions of P94A amicyanin are in progress to attempt to determine the effect of this mutation on electron transfer parameters for the reactions to and from the copper

center that may be correlated with the structural information presented in this paper.

ACKNOWLEDGMENT

Use of the Advanced Photon Source was supported by the U.S. Department of Energy, Office of Science, Office of Basic Energy Sciences, under Contract W-31-109-ENG-38. We thank the staff at BIOCARS for their assistance and equipment.

REFERENCES

1. Husain, M., and Davidson, V. L. (1985) An inducible periplasmic blue copper protein from *Paracoccus denitrificans*. Purification, properties, and physiological role, *J. Biol. Chem. 260*, 14626−14629.
2. Davidson, V. L. (2001) Pyrroloquinoline quinone (pqq) from methanol dehydrogenase and tryptophan tryptophylquinone (ttq) from methylamine dehydrogenase, *Adv. Protein Chem. 58*, 95−140.
3. Husain, M., and Davidson, V. L. (1986) Characterization of two inducible periplasmic c-type cytochromes from *Paracoccus denitrificans*, *J. Biol. Chem. 261*, 8577−8580.
4. Cunane, L. M., Chen, Z., Durley, R. C. E., and Mathews, F. S. (1996) X-ray crystal structure of the cupredoxin amicyanin from *Paracoccus denitrificans*, refined at 1.31 Å resolution, *Acta Crystallogr. D52*, 676−686.
5. Chen, L., Durley, R., Poliks, B. J., Hamada, K., Chen, Z., Mathews, F. S., Davidson, V. L., Satow, Y., Huizinga, E., and Vellieux, F. M. (1992) Crystal structure of an electron-transfer complex between methylamine dehydrogenase and amicyanin, *Biochemistry 31*, 4959−4964.
6. Chen, L., Durley, R. C., Mathews, F. S., and Davidson, V. L. (1994) Structure of an electron transfer complex: Methylamine dehydrogenase, amicyanin, and cytochrome c551i, *Science 264*, 86−90.
7. Machczynski, M. C., Gray, H. B., and Richards, J. H. (2002) An outer-sphere hydrogen-bond network constrains copper coordination in blue proteins, *J. Inorg. Biochem. 88*, 375−380.
8. Zhu, Z., Cunane, L. M., Chen, Z., Durley, R. C., Mathews, F. S., and Davidson, V. L. (1998) Molecular basis for interprotein complex-dependent effects on the redox properties of amicyanin, *Biochemistry 37*, 17128−17136.
9. Guss, J. M., Harrowell, P. R., Murata, M., Norris, V. A., and Freeman, H. C. (1986) Crystal structure analyses of reduced (CuI) poplar plastocyanin at six pH values, *J. Mol. Biol. 192*, 361−387.
10. Gray, K. A., Knaff, D. B., Husain, M., and Davidson, V. L. (1986) Measurement of the oxidation−reduction potentials of amicyanin and c-type cytochromes from *Paracoccus denitrificans*, *FEBS Lett. 207*, 239−242.
11. Davidson, V. L. (1990) Methylamine dehydrogenases from methylotrophic bacteria, *Methods Enzymol. 188*, 241−246.
12. Davidson, V. L., Jones, L. H., Graichen, M. E., Mathews, F. S., and Hosler, J. P. (1997) Factors which stabilize the methylamine dehydrogenase-amicyanin electron transfer protein complex revealed by site-directed mutagenesis, *Biochemistry 36*, 12733−12738.
13. Lim, L. W., Mathews, F. S., Husain, M., and Davidson, V. L. (1986) Preliminary X-ray crystallographic study of amicyanin from *Paracoccus denitrificans*, *J. Mol. Biol. 189*, 257−258.
14. Otwinowski, Z., and Minor, W. (1997) Processing of X-ray diffraction data collected by oscillation methods, *Methods Enzymol. 276*, 307−326.
15. Winn, M. D. (2003) An overview of the CCP4 project in protein crystallography: An example of a collaborative project, *J. Synchrotron Radiat. 10*, 23−25.
16. Brünger, A. T., Adams, P. D., Clore, G. M., DeLano, W. L., Gros, P., Grosse-Kunstleve, R. W., Jiang, J. S., Kuszewski, J., Nilges, M., Pannu, N. S., Read, R. J., Rice, L. M., Simonson, T., and Warren, G. L. (1998) Crystallography & NMR system: A new software suite for macromolecular structure determination, *Acta Crystallogr. D 54*, 905−921.
17. Sheldrick, G. M., and Schneider, T. R. (1997) Shelxl: High-resolution refinement, *Methods Enzymol. 277*, 319−343.
18. McRee, D. E. (1999) XtalView/Xfit—a versatile program for manipulating atomic coordinates and electron density, *J. Struct. Biol. 125*, 156−165.
19. Sun, D., and Davidson, V. L. (2003) Effects of engineering uphill electron transfer into the methylamine dehydrogenase-amicyanin-cytochrome c-551i complex, *Biochemistry 42*, 1772−1776.
20. Adman, E. T. (1991) Copper protein structures, *Adv. Protein Chem. 42*, 145−197.
21. Baker, E. N. (1988) Structure of azurin from *Alcaligenes denitrificans* refinement at 1.8 Å resolution and comparison of the two crystallographically independent molecules, *J. Mol. Biol. 203*, 1071−1095.
22. Petratos, K., Banner, D. W., Beppu, T., Wilson, K. S., and Tsernoglou, D. (1987) The crystal structure of pseudoazurin from *Acaligenes faecalis* S-6 determined at 2.9 Å resolution, *FEBS Lett. 218*, 209−214.
23. Nishiyama, M., Suzuki, J., Ohnuki, T., Chang, H. C., Horinouchi, S., Turley, S., Adman, E. T., and Beppu, T. (1992) Site-directed mutagenesis of pseudoazurin from *Alcaligenes faecalis* S-6; Pro80Ala mutant exhibits marked increase in reduction potential, *Protein Eng. 5*, 177−184.
24. Pascher, T., Karlsson, B. G., Nordling, M., Malmstrom, B. G., and Vanngard, T. (1993) Reduction potentials and their ph dependence in site-directed-mutant forms of azurin from *Pseudomonas aeruginosa*, *Eur. J. Biochem. 212*, 289−296.
25. Nar, H., Messerschmidt, A., Huber, R., van de Kamp, M., and Canters, G. W. (1991) Crystal structure analysis of oxidized *Pseudomonas aeruginosa* azurin at ph 5.5 and ph 9.0. A ph-induced conformational transition involves a peptide bond flip, *J. Mol. Biol. 221*, 765−772.
26. Libeu, C. A., Kukimoto, M., Nishiyama, M., Horinouchi, S., and Adman, E. T. (1997) Site-directed mutants of pseudoazurin: Explanation of increased redox potentials from X-ray structures and from calculation of redox potential differences, *Biochemistry 36*, 13160−13179.
27. Marcus, R. A., and Sutin, N. (1985) Electron transfers in chemistry and biology, *Biochim. Biophys. Acta 811*, 265−322.
28. Davidson, V. L., and Jones, L. H. (1996) Electron transfer from copper to heme within the methylamine dehydrogenase—amicyanin—cytochrome *c*-551i complex, *Biochemistry 35*, 8120−8125.
29. Brooks, H. B., and Davidson, V. L. (1994) Kinetic and thermodynamic analysis of a physiologic intermolecular electron transfer reaction between methylamine dehydrogenase and amicyanin, *Biochemistry 33*, 5696−5701.
30. Brooks, H. B., and Davidson, V. L. (1994) Free energy dependence of the electron transfer reaction between methylamine dehydrogenase and amicyanin, *J. Am. Chem. Soc. 116*, 11202−11202.
31. Brunger, A. T. (1992) Free *R* value: a novel statistical quantity for assessing the accuracy of crystal structures, *Nature 355*, 472−475.
32. Luzzati, V. (1952) Traitment statistique des erreurs dans la determination des structures cristallines, *Acta Crystallogr. 5*, 802−810.
33. Cruickshank, D. W. I. (1999) Remarks about protein structure precision, *Acta Crystallogr. D 55*, 583−601.
34. Kraulis, P. J. (1991) Molscript: A program to produce both detailed and schematic plots of protein structures, *J. Appl. Crystallogr. 24*, 946−950.
35. Merritt, E. A., and Bacon, D. J. (1997) Raster 3D: Photorealistic molecular graphics, *Methods Enzymol. 277*, 505−524.
36. Roussel, A., and Cambillau, C. (1991) Turbo-Frodo, in *Silicon graphics geometry partners directory 86*, Silicon Graphics, Mountain View, CA.
37. Carrell, C. J., Wang, X., Jones, L., Jarrett, W. L., Davidson, V. L., and Mathews, F. S. (2004) *Biochemistry 43*, 9381−9389.

BI049634Z